Open Access

Global selection appraisal study for heat pump system of electric vehicle based on energetic, economic, and environmental analysis

Kexin Li[1], Lingfeng Shi[1*], Yonghao Zhang[1], Yu Yao[1], Hua Tian[2] and Gequn Shu[1,2]

Abstract

The development of electric vehicles (EVs) exhibits rapid and remarkable progress nowadays, serving as a crucial route to accomplish the target of mitigating greenhouse gas emissions. As an integral part of the thermal management system oriented toward electric vehicles, the heat pump air conditioning system for electric vehicles is the result of a comprehensive choice that trades off the cooling and heating performance, environmental performance and economic cost. Particularly, different regions around the world suffer varying cooling and heating challenges due to the complicated climatic characteristics. Thus the most suitable refrigerant and system cycle structure may differ. This paper focuses on evaluating both the refrigerants and cycle structures to screen the most suitable choice. According to the climate conditions of different cities, the annual energy consumption, life cycle climate performance, and economic cost of the basic system (Base), two-stage compression system (TSC,IC), and vapor injection (VI) system with CO_2, R134a, and R1234yf refrigerants respectively, are quantitatively analyzed and evaluated. Subsequently, through comparative analysis, a comprehensive selection map for heat pump systems in electric vehicles worldwide is developed and the most suitable heat pump air conditioning system for each cites is determined. The results can provide a selection reference and decision-making for the air conditioning system of electric vehicles from regional considerations. It was found that the CO_2 $HPAC_{VI}$ was recommended for cold regions to meet both environmental and economic requirements. In warm region, the R1234yf $HPAC_{Base}$ system was recommended to be used. For regions transitioning from cold to warm climates, the R1234yf $HPAC_{VI}$ system was suggested. In hot region, the R1234yf AC system was recommended.

Keywords Electric vehicle, Heat pump, Refrigerants, Carbon emission, Life cycle cost

1 Introduction

With the increasing strictness of environmental awareness and greenhouse gas emission policies [1, 2], thepure battery electric vehicles (PBEVs) have rapidly developed as a promising solution to replace conventional internal combustion engine vehicles (ICEVs). Compared to ICEVs, PBEVs have an obvious advantage in terms of environmental friendliness, as they emit no harmful gases, including nitrogen oxides (NOx) and carbon monoxide (CO), as well as greenhouse gases, such as carbon dioxide (CO_2), during operation [3]. Therefore, promoting the development of PBEVs is crucial and has far-reaching implications.

The battery energy consumption in PBEVs is primarily determined by several factors, including the motor

*Correspondence:
Lingfeng Shi
slf@ustc.edu.cn
[1] Department of Thermal Science and Energy Engineering, University of Science and Technology of China, Hefei 230027, China
[2] State Key Laboratory of Engines, Tianjin University, Tianjin 300072, China

for propulsion, the air conditioning system for passenger comfort, and other electronic components. In particular, in winter, the driving range is significantly reduced due to the massive energy for cabin heating from the battery, leading to a phenomenon known as 'range anxiety', which is considered a major obstacle to the development of PBEVs in cold regions. Currently, the most commonly used heating method in PBEVs is the Positive Temperature Coefficient (PTC) heater, which is convenient and inexpensive but less efficient. Researchers have demonstrated that the use of a PTC heater in cold climates can result in a reduction of more than 50% in the driving range of PBEVs [4–6].

Researchers have shown interest in using heat pumps to address the problem of range anxiety in PBEVs during winter [7–10]. Unlike PTC heater, heat pump systems offer better heating efficiency, which significantly depends on weather conditions, and have a Coefficient Of Performance (COP) typically greater than 1. However, the choice of refrigerant is a crucial factor in the performance of heat pump systems, as it can significantly impact system efficiency and lead to environmental and cost-related issues. Therefore, the selection of an appropriate refrigerant requires careful consideration, especially given the worldwide and collective nature of PBEV development.

Currently, the mainstream refrigerant used in PBEV air conditioning systems is still R134a. The R134a air conditioning system offers a cooling performance advantage but less efficient for heating at cold weather and cannot meet the heating load under extreme cold weather conditions. Peng et al. [11] designed a R134a heat pump system for electric vehicles and tested its heating capacity at different temperatures. Their results indicated that the R134a heat pump air conditioning (HPAC) system could meet cabin heating demand with a high efficiency at -5 °C, as reflected by a COP of 4.55. However, the experiment did not involve lower temperatures. To investigate the heating performance of the R134a heat pump system at lower temperatures, Lee et al. [12] conducted experimental studies and found that the system could meet heating demand above -10 °C, but the PTC needed to be turned on below -10 °C due to a decrease in heating capacity and COP caused by the ambient temperature decline. However the Global Warming Potential (GWP) of R134a is 1300, indicating that excessive emissions of R134a could significantly intensify the greenhouse effect, contributing to global warming [13]. As a result, R134a is being phased out worldwide due to its high GWP of 1300. Alternatives such as R1234yf and CO_2 are being considered for future use. As these replacement refrigerants exhibit significant differences in terms of their heating/cooling performance, economy cost and environmental

friendliness. Therefore, careful evaluation of these alternatives is necessary to ensure the optimal selection of refrigerants for PBEVs.

In contrast to R134a, the potential replacement refrigerant R1234yf exhibits similar thermodynamic properties but with slightly reduced heating/cooling performance. Most notably, it has a significantly improved environmental profile due to its low GWP of 4 [14]. Li et al. [15] conducted experiments to compare the performance of R134a and R1234yf and found that at a condenser temperature of 40 °C and an evaporation temperature of 0 °C, the COP of R1234yf was 20% lower than that of R134a. Similarly, Zou et al. [16] built an electric vehicle heat pump air conditioning system to investigate the performance of R1234yf and R134a under different working conditions and found that the heating capacity and COP of R1234yf were approximately 10% lower than those of R134a. Additionally, Lee et al. [17] built R1234yf and R134a heat pump systems and tested them under cooling and heating conditions in a heat pump bench tester. The results showed that the COP of R1234yf was 0.8～2.7% lower than that of R134a.

Another natural refrigerant CO_2 with a GWP of 1 and Ozone Depletion Potential (ODP) of 0, has been proposed as a potential replacement, demonstrating superior environmental friendliness. Additionally, this refrigerant boasts advantages such as low cost, non-toxicity, non-flammability, and high latent heat [18, 19], making it an attractive option. Although CO_2 has unique thermophysical properties that make it advantageous for heating, its cooling performance is slightly inferior. Dong et al. [20] conducted a comparative analysis of the heating performance of a R134a heat pump system and a CO_2 heat pump system, demonstrating that at an ambient temperature of -10 °C, the COP of the CO_2 system was 80% higher than that of R134a at the same speed of 6000, with a heating capacity of 7378W (R134a, 3994W). Chen et al. [21] investigated the effects of outdoor temperature, outdoor air speed, indoor air volume, compressor speed, and EXV opening on the performance of a CO_2 heat pump, concluding that when the indoor and outdoor temperatures are -20 °C, the COP and heating capacity can reach 3.1 and 3.6 kW, respectively. Moreover, under outdoor, indoor, and outlet temperatures of -20 °C, 20 °C, and 40 °C, the COP was 1.7, demonstrating good heating performance in cold climates. Steven et al. [22] used a semi-theoretical cycle model to study the performance advantages of CO_2 and R134a automotive air conditioning systems, revealing that R134a has a better COP than CO_2, with the COP difference depending on compressor speed and ambient temperature. Ciro et al. [23] experimentally investigated the operating parameters and performance of R134a air conditioning systems and CO_2

Li *et al. Carbon Neutrality*   (2024) 3:16

Page 3 of 25

systems, demonstrating that the overall performance of R134a air conditioning systems consistently outperformed CO_2 (from 20 to 44% higher performance).

In general, the CO_2 refrigerant is better suited for cold regions due to its superior heating performance, while R134a and R1234yf refrigerants are more appropriate for hot regions [23–29]. However, determining the demarcation line for the most suitable refrigerant based on region presents a challenge. The weather conditions of each region differ due to variations in dimension and altitude. These differences result in varying heating and cooling hours and ranges, which significantly affect the annual energy consumption of HPAC in PBEVs. Considering the characteristics of those refrigerants, it becomes clear that each region has its own best-suited option. To determine the most appropriate refrigerant, it is essential to conduct comprehensive quantitative analyses, taking into account factors such as annual energy consumption, life cycle climate performance and economy cost.

In previous studies, Song et al. [30] and Liu et al. [31] conducted quantitative analyses on the regional applicability of CO_2 and R134a refrigerants. These studies were based on calculations of annual energy consumption, life-cycle carbon emissions, climate performance, and cost. However, their evaluations did not take into account the potential impact of improved system structures on heating and cooling performance and environmental performance. Therefore, to offer a more comprehensive and comparative assessment, this paper evaluates the global regional applicability of refrigerants and system cycle structures by conducting quantitative analysis of annual energy consumption, life cycle climate performance and cost. By considering both refrigerant and system cycle structure, this study aims to develop a selection map for air conditioning system used in PBEVs.

The paper is organized as follows: Sect. 2 introduces the heat pump air conditioning systems for each refrigerant, including both basic and improved systems. Additionally, theheating and cooling modes for each system are introduced and explained. The most commonly used system in PBEVs nowadays is also introduced as a comparison object. Section 3 presents the relevant calculation methods and formulas, including the simulation models for each system, the selected objective cities, the annual heating and cooling hours of each cities, and the calculation formulas for energy consumption, life cycle climate performance, and cost. Section 4 presents the heating and cooling performance of each system, the calculation results for energy consumption, carbon emissions, and cost for the objective cities, and provides the refrigerant suitability map. Finally, the major conclusions are presented in Sect. 5. This paper can serve as a reference for the selection of appropriate heat pump air conditioning systems for PBEVs all around the world.

2 System description

To provide a comprehensive comparison of various HPAC systems, this paper focuses on the system cycle structures and refrigerants that are currently being studied by researchers. These system cycle structures and refrigerants are chosen to cover a wide range of technologies and solutions, as shown in Table 1. Table 1 qualitatively summarizes the advantages and disadvantage of these combinations of refrigerants and system cycle structures and specific quantitative analysis is presented in the following content. By comparing and evaluating these systems and refrigerants, this paper aims to identify the most suitable HPAC system and refrigerant for PBEVs in each region. The detailed description of each system is as follows.

Table 1 The refrigerant and system cycle structure are discussed in this paper [32–36]

System	Brief description	Advantage	Disadvantage
CO_2 HPAC$_{Base}$	Base cycle	Good in heating; Green	Poor in cooling
CO_2 HPAC$_{TSC,IC}$	Two-Stage Compression with intercooling	Excellent in heating; Green	expensive
CO_2 HPAC$_{VI}$	Vapor injection	Superb in heating; Green	Very expensive
R134a AC	PTC heating	cheap	Extremely poor in heating; Extremely Non-eco-friendly
R134a HPAC$_{Base}$	Base cycle	Very Good in cooling	Poor in heating; Non-eco-friendly
R134a HPAC$_{VI}$	Vapor injection	Good in heating	Expensive; Non-eco-friendly
R1234yf AC	PTC heating	cheap	Extremely Poor in heating Non-eco-friendly
R1234yf HPAC$_{Base}$	Base cycle	Good in cooling Moderately eco-friendly	Poor in heating
R1234yf HPAC$_{VI}$	Vapor injection	Good in heating; Moderately eco-friendly	expensive

Li *et al. Carbon Neutrality* (2024) 3:16

Page 4 of 25

(a) R134a/R1234yf AC

(b) R134a/R1234yf HPAC$_{Base}$

(c) R134a/R1234yf HPAC$_{VI}$

(d) CO$_2$ HPAC$_{SSC}$

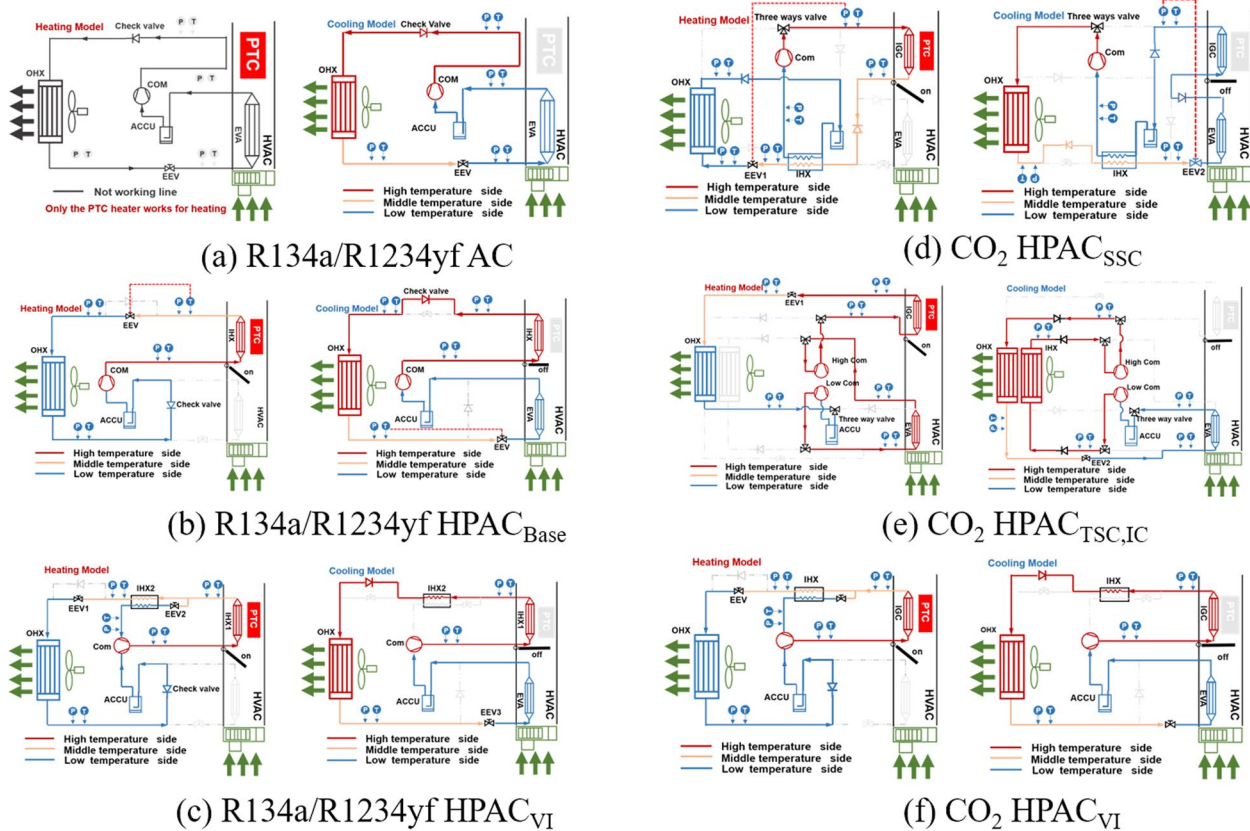**(e) CO$_2$ HPAC$_{TSC,IC}$**

(f) CO$_2$ HPAC$_{VI}$

Fig. 1 The schematic diagram of systems discussed in this paper

2.1 R134a/R1234yf refrigeration air condition system

Figure 1(a) presents the schematic of the R134a and R1234yf refrigeration air condition system (R134a/R1234yf AC). The system of R134a and R1234yf is compatible due to their close thermodynamic properties, and can be used interchangeably with the same components and lube oil. Therefore, they are introduced together in this study. The system comprises a compressor, an outdoor heat exchanger (OHX), an indoor evaporator (EVA), an electronic expansion valve (EEV), and an accumulator. During the heating mode, the PTC heater is activated to heat the cold air, which is then delivered to the cabin. On the other hand, the air conditioning system remains inactive. During summer, the R134a/R1234yf air conditioning system cools the air, and hence the system is referred to as R134a/R1234yf AC+PTC system. The system is characterized by its simple structure, low cost, and wide application, but suffers from inefficiency.

2.2 R134a/R1234yf base heat pump air conditioning system

Figure 1(b) show the schematic of R134a/R1234yf base heat pump air conditioning system (R134a/R1234yf HPAC$_{Base}$).

This system mainly includes a compressor, an indoor heat exchanger (IHX), an evaporator (EVA) and an accumulator (ACCU), two electronic expansion valves (EEV), outdoor heat exchanger (OHX). The abbreviation HPAC stands for a system can heat the air in heat pump and cool the air in air conditioning.

Based on the valve's switching, the system can alternate between cooling and heating functions. It's important to note that when in cooling mode, the damper on the indoor side is closed, preventing the IHX from exchanging heat with the air. However, in heating mode, the damper opens, allowing the air to be heated. The refrigerant entering the compressor has a superheat of 0 K, thanks to separation in the ACCU, necessitating system control by managing the refrigerant's subcooling as it exits the OHX /IHX. The target subcooling is set at 10 K.

2.3 R134a/R1234yf vapor injection heat pump air conditioning system

Figure 1(c) display the configuration diagrams of R134a/R1234yf vapor injection heat pump air conditioning system (R134a/R1234yf HPAC$_{VI}$) designed for improving heating performance at extremely low temperatures.

Li *et al. Carbon Neutrality*   (2024) 3:16

Page 5 of 25

This system comprises a vapor injection compressor, an indoor heat exchanger (IHX1), an intermediate heat exchanger (IHX2), an outdoor heat exchanger (OHX), an accumulator (ACCU), three electronic expansion valves (EEV), and an evaporator (EVA). Specifically, EEV2 in the vapor injection path is used to control the timing and occurrence of refrigerant injection into the compressor.

In heating mode, the refrigerant, which is at high temperature and pressure, is initially directed to IHX1 to exchange heat with and warm the fresh air. After exiting the IHX1, the refrigerant flow is divided into two parts: the main path and the injection path. Specifically, the refrigerant in the injection path is expanded by EEV2 into a two-phase flow, then it is heated back to saturated vapor in IHX2 before being rerouted to the compressor. Meanwhile, the refrigerant in the main path undergoes supercooling in IHX2, then is expanded and depressurized by EEV1 into a two-phase flow. This refrigerant then passes through the OHX to absorb heat from the outdoor air before entering the ACCU, where the liquid is separated before the mixture returns to the compressor.

In cooling mode, the branch electronic expansion valve is closed due to no significant improvement in performance and to reduce the system's complexity; the system loop configuration remains the same as that of the base system.

2.4 CO_2 single-stage compression heat pump air conditioning system

Figure 1(d) illustrates the configuration diagrams of CO_2 single-stage compression heat pump air-conditioning system (CO_2 $HPAC_{SSC}$), which consists of a CO_2 compressor, a three-way valve, an indoor gas cooler (IGC), an evaporator (EVA), an outdoor heat exchanger (OHX), two electronic expansion valves (EEV), and an intermediate heat exchanger (IHX). The system is designed to achieve the switching of cooling and heating functions through the three-way valve.

To enhance the system performance, An IHX is used to supercool the CO_2 before it enters the EEV and superheat the CO_2 before enters compressor preventing the liquid shock. But this may increase the compressor discharge temperature. The discharge pressure is controlled by adjusting the opening of the EEV, which allows the system to operate at an optimal pressure and achieve efficient operation.

2.5 CO_2 two-stage compression with intercooling heat pump air conditioning system

The schematic and enthalpy diagram of a CO_2 two-stage compression with intercooling heat pump air-conditioning system (CO_2 $HPAC_{TSC,IC}$) are presented in Fig. 1(e). The system consists of two CO_2 compressors, an indoor gas cooler (IGS), an evaporator (EVA), four three-way valves, an inter heat exchanger (IHX), an outdoor heat exchanger (OHX), two electronic expansion valves (EEV), and an accumulator (ACCU).

In heating mode, CO_2 is compressed to the middle-pressure at the low-stage compressor and then enters the EVA to heat the fresh cold air. And then the CO_2 is compressed into high-pressure and high temperature by the high-stage compressor and enters the IGC to provide additional heating to the air. After being throttled by EEV1, the CO_2 two-phase flow moves to the OHX to absorb heat from the outdoor cold air, and then passes through the ACCU to separate the liquid before returning to the low-stage compressor. In cooling mode, the system operates similarly, but the intermediate heat exchange occurs in the IHX outside the vehicle.

2.6 CO_2 vapor injection heat pump air conditioning system

In Fig. 1(f), the schematic diagram of a CO_2 vapor injection heat pump air-conditioning system (CO_2 $HPAC_{VI}$) are presented. The system consists of a vapor injection CO_2 compressor, an indoor gas cooler (IGS), an evaporator (EVA), an inter heat exchanger (IHX), an outdoor heat exchanger (OHX), three electronic expansion valves (EEV), and an accumulator (ACCU). The system operates similarly to an R134a/R1234yf HP_{VI}, as illustrated in the figure, with the only difference being the specific components used in the CO_2 system.

3 Methodology

This section provides a detailed introduction to the overall ideas and calculation method, along with a logical flow chart of the calculations depicted in Fig. 2, to facilitate a better understanding of the topic at hand.

3.1 Simulation model of each system

The objective of constructing simulation models is to determine the energy consumption of each HVAC system at different heating and cooling temperatures to facilitate subsequent calculations of carbon emissions and economic cost. The heating and cooling load of the cabin is influenced by various factors, including ambient temperature, car speed, and solar radiation, with ambient temperature being the most critical. Accurately calculating the heating and cooling load and power consumption of the HVAC system under such diverse factors are challenging and error-prone task. Therefore, in this study, the models of each heat pump air conditioning system are developed using the AMESIM platform.

The simulation model incorporates the structure and performance parameters of each component from actual systems, and the simulation model, which includes the structural parameters of each component as shown in
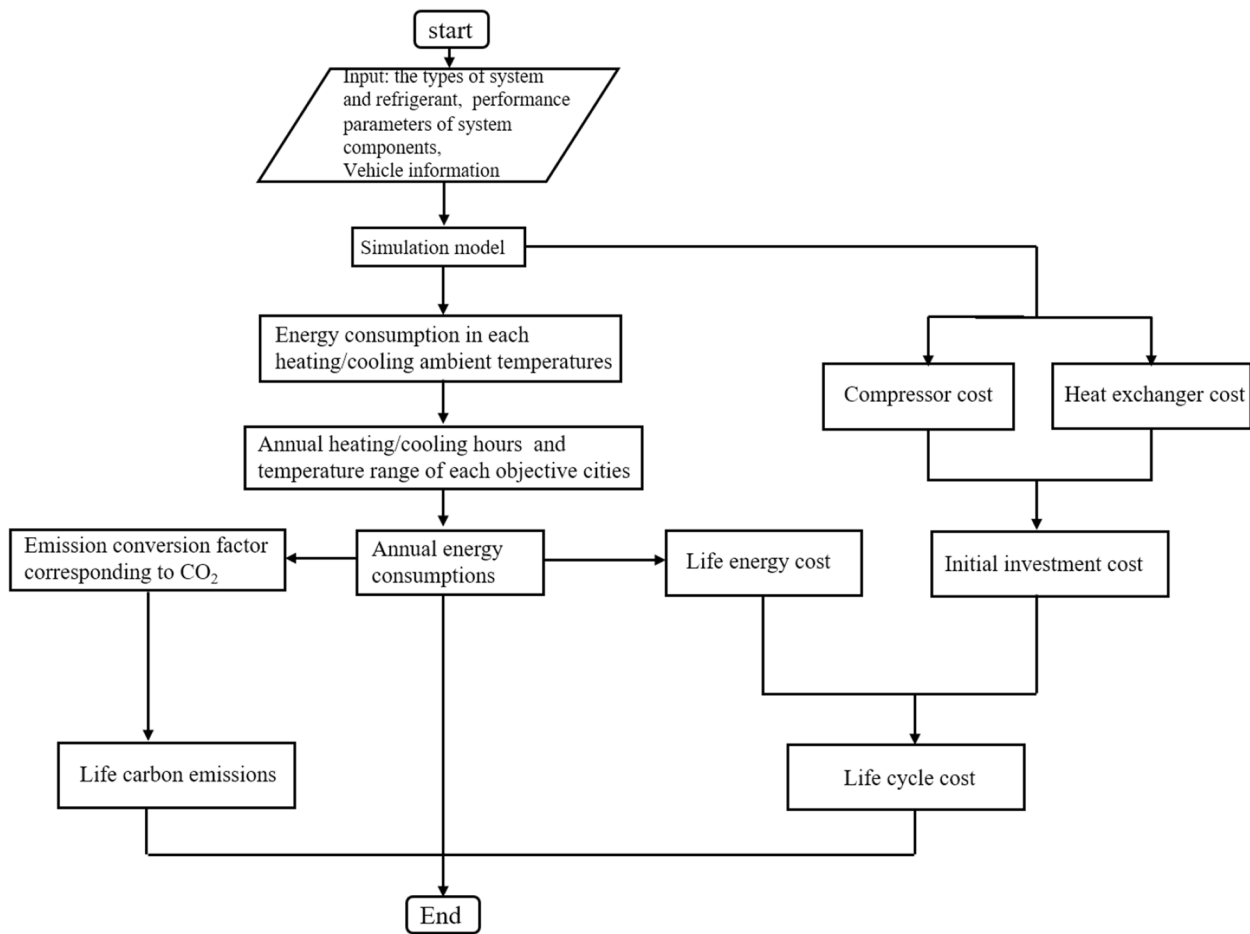
Fig. 2 The logical flow chart of the calculation

Table 2 The key parameters of the component structure of each system

Component	CO$_2$ system	R134a/R1234yf system
Compressor	Displacement:8cm3	Displacement:34cm3
	Rorate speed:600~7000r/min	Rorate speed:600~7000r/min
Indoor gas cooler	Aluminum	Aluminum
	Microchannel heat exchanger	Microchannel heat exchanger
	Size:350mm X 403mm X 25mm	Size:225mm X 125mm X 27mm
Indoor evaporator	Aluminum	Aluminum
	Microchannel heat exchanger	Plate and fin heat exchanger
	Size:200mm X 232mm X 30mm	Size:200mm X 232mm X 30mm
Outdoor heat exchanger	Aluminum	Aluminum
	Microchannel heat exchanger	Microchannel heat exchanger
	Size:550mm X 403mm X 16mm	Size:550mm X 403mm X 16mm
Electronic expansion valve	Diameter for Refrigeration:5.5mm	Diameter for Refrigeration:5.5mm
	Diameter for Heating: 9.2mm	Diameter for Heating: 9.2mm
Intermediate heat exchanger	Copper coaxial tubular type length:1.5m	Copper coaxial tubular type length:1 m
Accumulator	Volume:800cm3	Volume:800cm3

Table 2. The model can accurately calculate the cabin heating and cooling load and HPAC's power consumption under different driving road conditions. To obtain more accurate and persuasive results, the model considers boundary conditions such as ambient temperature and cabin geometry parameters. Furthermore, the model incorporates control methods for the efficient operation of HPAC systems. For instance, a proportional-integral-derivative (PID) controller is employed to regulate the compressor speed and maintain the cabin temperature at the setpoint.

To simplify the theoretical calculation of the system, the following assumptions are made:

(1) All components in the system are assumed to be steady state.
(2) The irreversibility of the compression process in the compressor is considered, taking into account the isentropic efficiency and volumetric efficiency which are both dependent on the compressor's pressure ratio.
(3) All the refrigerant pressure drops and heat losses to the environment are neglected.
(4) The throttling processes in EEV are isenthalpic.
(5) The refrigerant flow in the system is characterized as continuous.

The compressor is the core component of the heat pump air conditioning system, which is responsible for the compression and transportation of refrigerant. In the compressor compression process, the low temperature and pressure refrigerant is compressed into high temperature and pressure, and the mechanical work consumed by itself is converted into the enthalpy energy of the refrigerant. In the compression process, the pressure ratio, the mass flow rate, power consumption, isentropic efficiency and are used to describe the working performance and state of the compressor.

The equation for the compressor pressure ratio and theoretical flow rate [37] in the simulation system is as follows (1) and (2):

$$tau = \frac{P_{dis}}{p_{suc}} \tag{1}$$

$$m_f = \eta_v \rho_{suc} N disp \tag{2}$$

where:
tau: the pressure ratio;
P_{dis}: discharge pressure, pa;
p_{suc}: suction pressure, pa;
m_f: the mass flow rate of refrigerant, kg·s^{-1};
η_v: volumetric efficiency;

ρ_{suc}: suction density, kg·m^{-3};
N: rotary speed of the compressor, rev·s^{-1};
$disp$: compressor displacement, m^3.
η_v is the volumetric efficiencies of CO_2 [37]and the volumetric efficiencies of R134a/R1234yf [38, 39]

The isentropic efficiency is used to compute the enthalpy increase through the compressor. The isentropic efficiency can be expressed as follow (3):

$$\eta_{is} = \frac{h_{dis} - h_{suc}}{h_{dis} - h_{suc}} \tag{3}$$

where:
η_{is}: isentropic efficiency.
h_{dis}: isentropic discharge specific enthalpy, J·kg^{-1};
h_{dis}: discharge specific enthalpy, J·kg^{-1};
h_{suc}: suction specific enthalpy J·kg^{-1};
η_{is} is the isentropic efficiencies of CO_2 [37]and the volumetric efficiencies of R134a/R1234yf [38, 39].

The compression process is power-consuming, and the power consumption of compressor is calculated as follows (4):

$$W = m_f(h_{dis} - h_{suc}) \tag{4}$$

where:
W: the power consumption of compressor, W.

The heating and cooling load of the system are calculated as follow (5):

$$Q_{heating} = m_f(h_{ref,in} - h_{ref,out})$$
$$Q_{cooling} = m_f(h\prime_{ref,out} - h\prime_{ref,in}) \tag{5}$$

where:
$Q_{heating}$: the heating load, W;
$h_{ref,in}$: enthalpy of refrigerant at the inlet of the indoor heat exchanger, J·kg^{-1};
$h_{ref,out}$: enthalpy of refrigerant at the outlet of the indoor heat exchanger, J·kg^{-1};
$Q_{cooling}$: the cooling load, W;
$h\prime_{ref,out}$: enthalpy of refrigerant at the outlet of the indoor evaporator, J·kg^{-1};
$h\prime_{ref,in}$: enthalpy of refrigerant at the inlet of the indoor evaporator, J·kg^{-1};

The COP [40, 41] is a numerical index that indicates the performance of the heat pump air conditioning system, and its calculation formula is as follows (6):

$$COP = \frac{Q}{W} \tag{6}$$

where:
COP: Coefficient Of Performance;
Q: the heating load or the cooling load, W;
W: the compressor power consumption, W;

Li *et al. Carbon Neutrality* (2024) 3:16

Page 8 of 25

Corresponding to the system schematic diagram in Sect. 2, the calculation principle of COP for each system is the same as (6), but there are slight differences in parameter values. The performance calculation methods for each system are detailed in Table 3.

The modeling of the heat transfer process of the system's heat exchanger is also important. The main heat exchange process of the heat exchanger is mainly composed of two: the heat exchange of the refrigerant and the inner tube of the heat exchanger microchannel, and the heat exchange of the air and the heat exchanger fins.

Heat transfer between the refrigerant and the inner tube of the microchannel of the heat exchanger is calculation as follows (7):

$$Q_{ref} = h_{ref} A_{in} (T_{ref} - T_{wall}) \tag{7}$$

where:

Table 3 The calculation equations of COP for each system [37]

System	Equation
R134a/R1234yf HPAC$_{Base}$	$Q_{heating} = M_f * (h_2 - h_3)$
	$Q_{Cooling} = M_f * (h_1 - h_4)$
	$W = M_f * (h_2 - h_1)$
	$COP_{heating} = Q_{heating}/W$
	$COP_{Cooling} = Q_{Cooling}/W$
R134a/R1234yf HPAC$_{VI}$	$Q_{heating} = M_f * (h_4 - h_5)$
	$W_{heating} = (M_f - M_{VI}) * (h_2 - h_1) + M_f * (h_4 - h_3)$
	$COP_{heating} = Q_{heating}/W_{heating}$
	$Q_{Cooling} = M_f * (h_1 - h_4)$
	$W_{Cooling} = M_f * (h_2 - h_1)$
	$COP_{Cooling} = Q_{Cooling}/W_{Cooling}$
CO$_2$ HPAC$_{ssc}$	$Q_{heating} = M_f * (h_3 - h_4)$
	$Q_{Cooling} = M_f * (h_3 - h_4)$
	$W = M_f * (h_3 - h_2)$
	$COP_{heating} = Q_{heating}/W$
	$COP_{Cooling} = Q_{Cooling}/W$
CO$_2$ HPAC$_{TSC,IC}$	$Q_{heating} = M_f * (h_4 - h_5)$
	$Q_{Cooling} = M_f * (h_4 - h_5)$
	$W = M_f * ((h_2 - h_1) + (h_4 - h_3))$
	$COP_{heating} = Q_{heating}/W$
	$COP_{Cooling} = Q_{Cooling}/W$
CO$_2$ HPAC$_{VI}$	$Q_{heating} = M_f * (h_4 - h_5)$
	$W_{heating} = (M_f - M_{VI}) * (h_2 - h_1) + M_f * (h_4 - h_3)$
	$COP_{heating} = Q_{heating}/W_{heating}$
	$Q_{Cooling} = M_f * (h_1 - h_4)$
	$W_{Cooling} = M_f * (h_2 - h_1)$
	$COP_{Cooling} = Q_{Cooling}/W_{Cooling}$

Q_{ref}: Heat exchange between the refrigerant and heat exchanger, W;

h_{ref}: Coefficient of internal convection heat transfer of refrigerant, J·m^{-2}·K^{-1};

A_{in}: heat exchange area between the refrigerant and heat exchanger, m^2;

T_{ref}: temperature of refrigerant, K;

T_{wall}: inner tube of the microchannel, K.

Heat transfer between air and heat exchanger fins is calculated as follow:

$$Q_{air} = h_{air} A_{out} (T_{wall} - T_{air}) \tag{8}$$

where:

Q_{air}: Heat transfer between air and heat exchanger fins, W;

h_{air}: Air convection heat transfer coefficient, J·m^{-2}·K^{-1};

A_{out}: Air convection heat transfer area, m^2;

T_{air}: temperature of air, K.

The convective heat transfer coefficient of refrigerant and air is referred to the Gnielinski [42] and shah [43] correlation formula, as follows (9, 10 and 11):

For single-phase heat transfer:

$$Nu_{ref} = \begin{cases} \dfrac{(Re - 1000) * Pr * \frac{f}{8}}{1 + 12.7 * \sqrt{\frac{f}{8}} * (Pr^{\frac{2}{3}} - 1)} & (2300 \le Re \le 10^6, 0.5 \le Pr \le 2000) \\ 4.36 & (Re \le 2300) \end{cases} \tag{9}$$

For phase change heat transfer:

$$Nu_{ref} = 0.023 Re^{0.8} Pr^{0.4} \tag{10}$$

For air side surface heat transfer:

$$Nu_{air} = 0.023 Re_{air}^{0.8} Pr_{air}^{0.33} \tag{11}$$

where:

Nu: Nussel number;

Re: Reynolds number;

Pr: The Planck number.

During the simulation process, external condition parameters, such as ambient temperature, air mass flow rate, pressure, and humidity, are specified and input into the air side of the out/indoor heat exchanger, while internal parameters such as vehicle speed and solar radiation intensity are input into the cabin integration module. The simulation models developed using the AMESIM platform exhibit high precision and accuracy. To validate the models, simulated results are compared with experimental results obtained from the CO$_2$ single-stage compression system [44], as shown in Fig. 3. The average error is less than 3%, indicating the high accuracy of the simulation model. Based on the similarity in the methodology, it
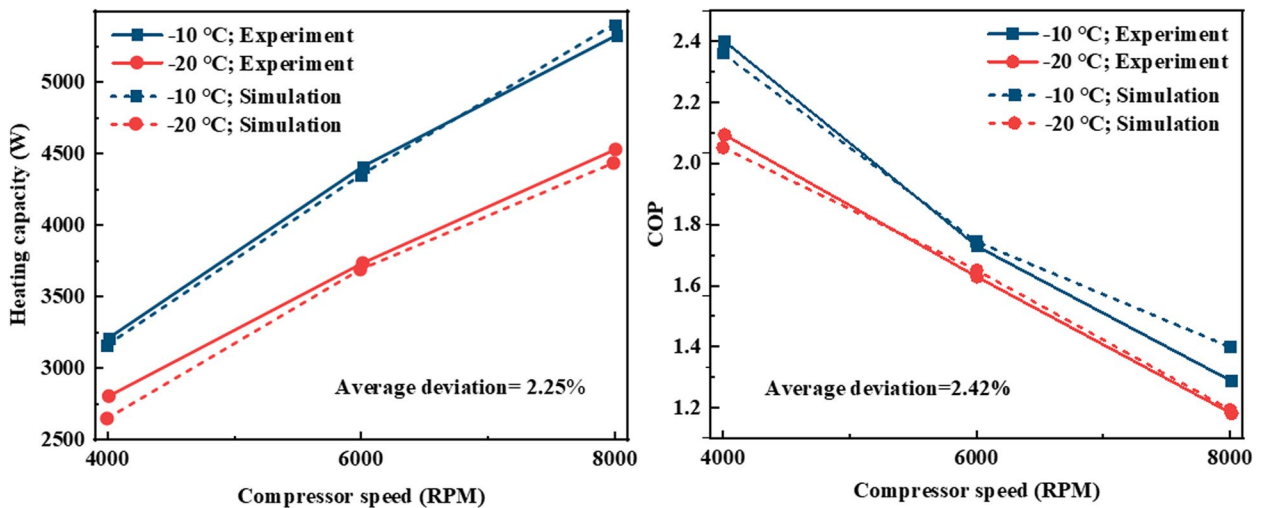
Fig. 3 The relative error of the simulation and experiment

is reasonable to infer that the simulation model of R134a/R1234yf is equally accurate.

3.2 Selection of electric vehicle cabin model
The cabin structural parameters are crucial factors that mainly determine the annual energy consumption. In the paper, a BYD Qin EV is employed to evaluate the heating/cooling loads under different conditions. The structural parameters of the vehicle are presented in Table 4.

3.3 Selection of objective cities
This paper considers 140 cities worldwide as the reference city. Those chosen cities equally distributed aiming to more comprehensive results. Cities in different regions

Table 4 The detailed structure parameters of the BYD Qin electric vehicle

Items	Parameters	Items	Parameters
Vehicle length (mm)	4765	External exchange surface (m^2)	12
Vehicle width (mm)	1837	Solar flux ($W \cdot m^{-2}$)	300
Vehicle high (mm)	1495	Solo flux absorption coefficient	0.45
Wall thermal capacity($J \cdot k^{-1}$)	7000	Internal aerodynamic coefficient	20
Internal exchange surface (m^2)	10		
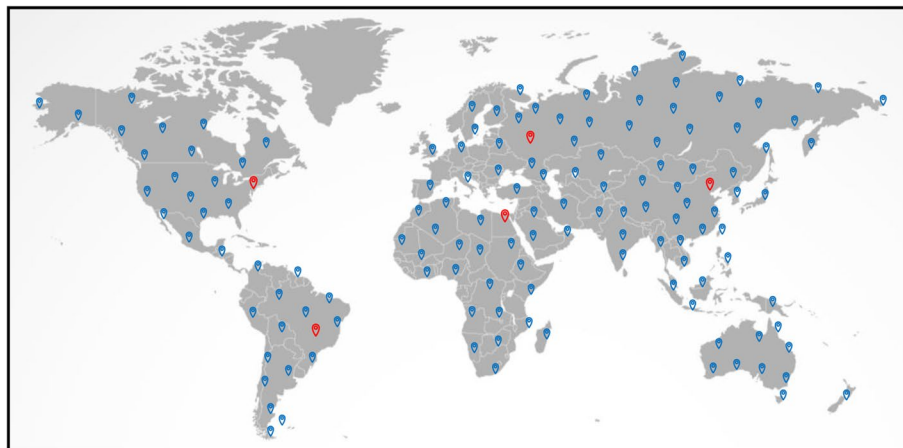
Fig. 4 Location distributions of objective cities

Li *et al. Carbon Neutrality*   (2024) 3:16

Page 10 of 25

have huge differences in annual heating and cooling energy consumption of HPAC due to different climate conditions such as ambient temperature, and energy consumption differences become the basis for carbon emissions and economic analysis. The objective cities are marked on the map in Fig. 4 by red and blue flags. To provide a comprehensive analysis, results for five cities, namely, Beijing, Moscow, Brasilia, Washington, and Cairo, are presented as examples, while the results for other cities are shown on the map.

3.4 Annual statistics of the heating and cooling time in objective cities

The annual energy consumption of HPAC system is strongly dependent on its operating hours and the corresponding ambient temperature. The longer the vehicle runs under harsher ambient temperatures, the higher the energy consumption of the HPAC system throughout the year. Therefore, it is crucial to date the annual operating hours of the HPAC system under different ambient temperatures accurately.

This paper selected the taxis as research object, given their extensive usage and comparatively longer driving duration, which makes them more representative. However, considering the large temperature difference between day and night and considering that the majority

of taxis operate primarily during the day with significantly less activity at night, it would be inaccurate and unreasonable to count all 24 h as heating/cooling times. Such a method would likely result in overestimating the annual power consumption, as vehicles do not operate around the clock.

Considering that China has the largest number of electric taxis, choosing them as reference object aligns with the statistical principle of a large sample size. Therefore, this study uses the travel characteristics of China's electric taxis as the reference for vehicle running models. The 2021 Chinese electric taxi running characteristics is shown as the Fig. 5. The average run time of electric taxis is 8.17 h, mainly concentrated between 6 and 19 o'clock. Based on this, the study selects an 8.17-h window with the highest travel frequency as the key operating time characteristic for the vehicle model. So, this paper selected 7–9, 10–14 and 16–18 o'clock as the research period. The average run mileage is 201.88 km, and the driving speed of vehicle model is maintained at 24.7 km/h. Considering the global time differences, the research period selected in this paper might align with nighttime in other regions. To address this, the study ensures that the selected research period corresponds to local time by applying time difference adjustments.
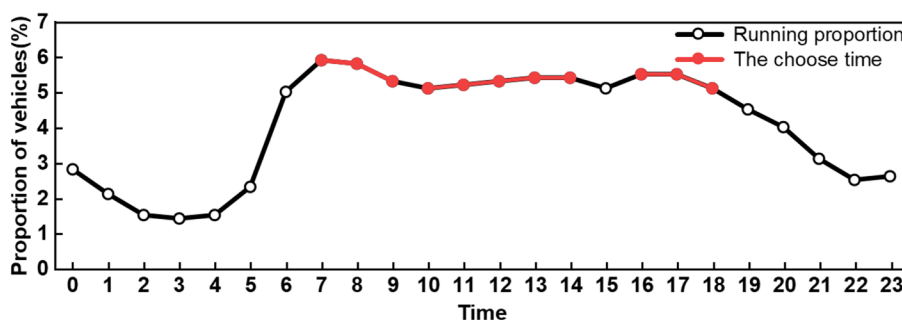
(a) Running timetable
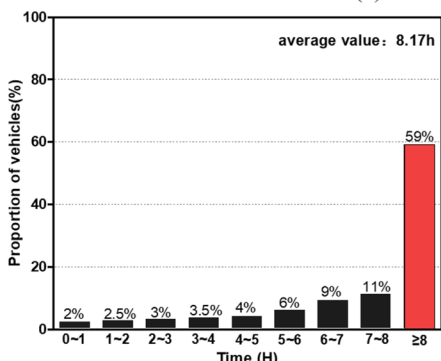
(b) Average mileage
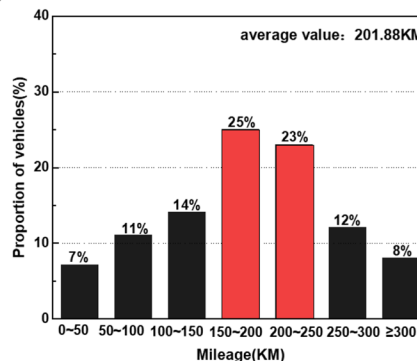
(c) Average mileage

Fig. 5 Daily driving characteristics of electric vehicles

Li *et al. Carbon Neutrality*   (2024) 3:16

Page 11 of 25
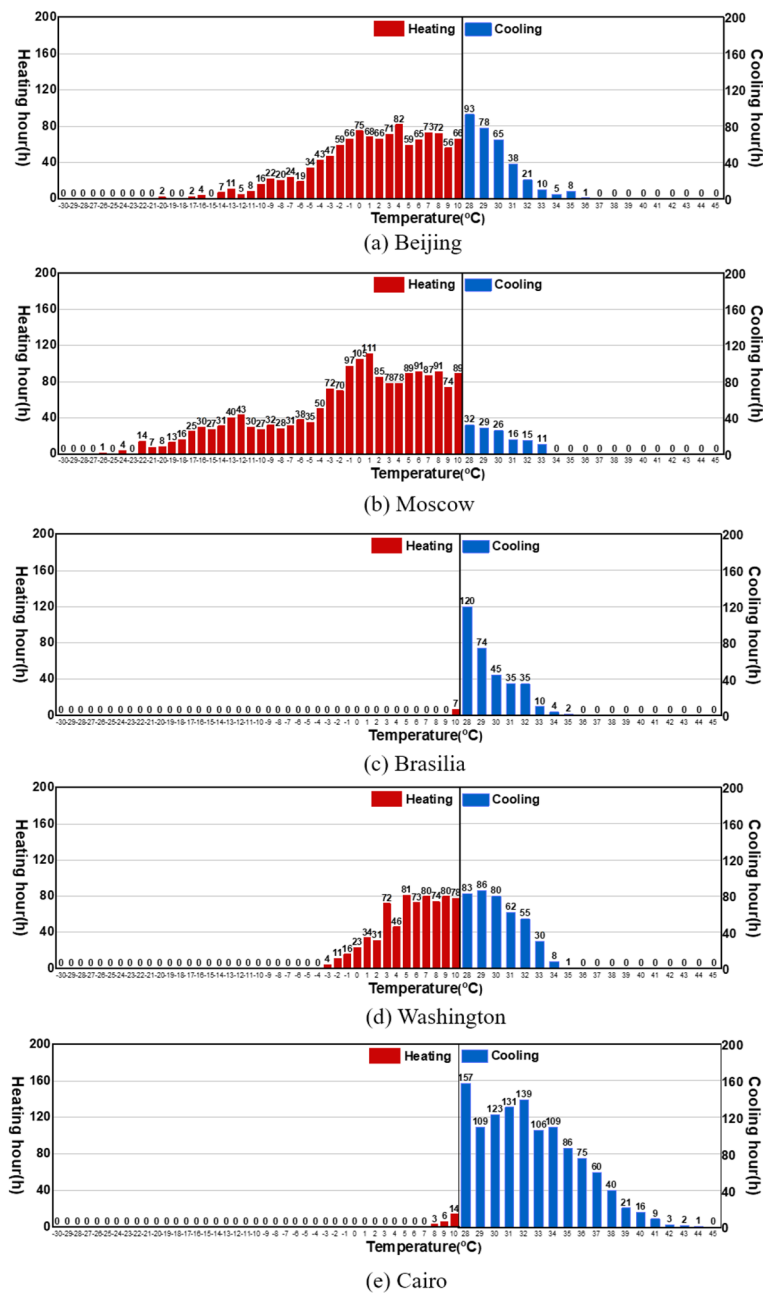
Fig. 6 The heating/cooling times of sample cities

To capture the ambient temperature corresponding to the operating times, this paper used the professional meteorological data APP, Wheat. Wheat is a professional scientific data system that integrates agricultural production, meteorology, environmental monitoring, and other multi-plate content. This paper queries and invokes the hourly temperature data of each city throughout the year in Wheat.

In this paper, the heating function of the HPAC is turned on when the ambient temperature is lower than 10 °C, and the cooling function is turned on when the ambient temperature is higher than 28 °C. The HPAC is not turned on in other temperature ranges. The statistical results of the annual heating/cooling hours in sample cities are presented in Fig. 6.

Figure 6 demonstrates that the annual heating/cooling hours differ significantly among different cities due

Li *et al. Carbon Neutrality*   (2024) 3:16

Page 12 of 25

to variations in latitude. Therefore, the choice of refrigerant and HPAC system should be based on the region to achieve lower energy consumption, carbon emissions and cost. For instance, in Cairo, the heating hours are much less than the cooling hours, and the heating temperature is concentrated at 8 °C, while the cooling temperature is concentrated below 40 °C. Therefore, using R134a/R1234yf refrigerant as the working fluid in the HPAC system is more suitable. In contrast, in Moscow, the heating time is considerably longer than the cooling time, and the heating temperature distribution is more even. Therefore, refrigerant CO_2 is more suitable for use in this city. The heating/cooling hours and range are the primary factors to consider when selecting the refrigerant and system. However, defining these boundaries presents a difficult task.

3.5 Annual energy consumption calculation method
After collecting statistics on the cooling and heating times of each province and simulating the power consumption of each heat pump system under different ambient temperatures, it is possible to calculate the annual air conditioning energy consumption of the vehicle in each city. The calculation formula is as follow (12):

$$W_{total} = \sum_{T=-30}^{T=10} W_{Heating} \times T_{Heating} + \sum_{T=28}^{T=45} W_{Cooling} \times T_{Cooling}$$
(12)

where:

$T_{heating}$: the Duration at each heating temperature, h;
$T_{cooling}$: the Duration at each cooling temperature, h;

3.6 Environmental performance calculation method
The life Cycle Climate Performance (LCCP) [45] is an index that shows the carbon emission discharged over the life cycle of both refrigerant and system. It includes two sources of carbon emission: direct and indirect. The former refers the equivalent carbon emissions form refrigerant leaks and the latter represents the equivalent carbon emissions form the power consumption.

The Life Cycle Climate Performance of each HPAC system can be calculated as follows:

$$LCCP_{total} = LCCP_{direct} + LCCP_{indirect}$$
(13)

$$LCCP_{direct} = [L \times n + R \times (1 - \alpha)] \times (GWP + adp.GWP)$$
(14)

$$LCCP_{indirect} = L \times E_\alpha \times \beta$$
(15)

where:

L: Average lifetime of equipment, year;
n: annual leakage rate

Table 5 The main environmental parameters of CO_2, R134a and R1234yf

Items	CO_2	R134a	R1234yf
Average lifetime (year)	15	15	15
Leakage rate	10%	10%	10%
Recovery rate	0	0	0
Carbon production rate (kg·kWh^{-1})	0.997		
GWP	1	1300	4
Adp. GWP	0	1.6	3.3

Table 6 Equations of initial investment cost for each system

system	Equation
R134a/R1234yf AC	$IIC = C_{com} + C_{eva} + C_{cond} + C_{add}$
R134a/R1234yf HPAC$_{Base}$	$IIC = C_{com} + C_{eva1} + C_{cond} + C_{eva2} + C_{add}$
R134a/R1234yf HPAC$_{VI}$	$IIC = C_{com1} + C_{com2} + C_{eva1} + C_{cond} + C_{eva2} + C_{add}$
CO_2 HPAC$_{SSC}$	$IIC = C_{com} + C_{eva1} + C_{cond} + C_{eva2} + C_{IHX} + C_{add}$
CO_2 HPAC$_{TSC,IC}$	$IIC = C_{com1} + C_{com2} + C_{eva1} + C_{cond} + C_{IHX} + C_{eva2} + C_{add}$
CO_2 HPAC$_{VI}$	$IIC = C_{com1} + C_{com2} + C_{eva1} + C_{cond} + C_{eva2} + C_{add}$

R: the residual amount of refrigeration in retired equipment, kg;
α: the refrigeration recovery rate
GWP: global warming potential
$adp.GWP$: GWP of atmospheric degradation product of the refrigerant
E_α: the energy consumption per year, kWh·year^{-1}
β: the amount of CO_2 emissions for 1 kWh energy generation, kg·kWh^{-1}

Those parameters [46, 47] of CO_2, R134a and R1234yf systems could be found in Table 5.

3.7 The life cycle cost calculation method
In this paper, the economic analysis comprises two components: the initial investment cost (IIC) and the life energy cost (LEC). The IIC represents the total cost of all system components, including the Compressor, gas cooler, evaporator, and additional equipment (such as throttle valve, pipe lines, etc.). The IIC for each system is presented in Table 6. The additional equipment cost is considered as 15% of the major equipment cost [48]. And the components cost is closely related to factors such as industry maturity, region and time.CO_2 HPAC systems are currently in the early stages of development, with limited large-scale production of CO_2 compressors and minimal literature on the economic analysis of CO_2 heat pump systems used in PBEV. Therefore, the IIC of CO_2 systems is evaluated in a manner similar to Song et al. [30].

Table 7 Equations for cost of compressors and heat exchangers [31]

Equipment	Correlation	Description
R134a/R1234yf compressor	$C_{COM,R134a} = 758.18W^{0.8728}$	W and A are the rated power of compressor and the area of heat exchanger
Finned tube heat exchanger	$C_{HE,FT} = 331.7A^{0.9390}$	
Double-tube heat exchanger	$CHE,DT = 1874.4A^{0.9835}$	

In this paper, the cost of each component of the CO_2 heat pump system is obtained through consulting the manufacturer and online survey. However, the electric vehicle R134a and R1234yf heat pump industry is mature, and the component cost is stable. Therefore, the capital costs for compressors and heat exchangers in R134a/R1234yf systems are determined using the formulas specified in Table 7. In addition, all heat exchangers in this study utilize finned tube heat exchangers, with the component structures presented in Table 2. The LEC corresponds to the annual power consumption cost. The calculation formula of economic analysis is as follows (16) and (17):

$$C_{tatal} = ICC + LEC \tag{16}$$

$$LEC = W_{tatal} \times C_{ele} \times L \tag{17}$$

where:
C_{tatal}: Total life cycle investment, CNY;
ICC: the initial investment cost, CNY;
LEC: life energy cost, CNY;
C_{ele}: the unit electricity cost factor, CNY·kWh^{-1};
L: lifetime of equipment, year.

3.8 The comprehensive evaluation criteria
After performing rigorous quantization calculations on the annual power consumption, life cycle climate performance, and life total cost, a comprehensive criterion is required to holistically evaluate these three parameters

holistically. The criterion here is based on the idea that the carbon emission is transformed into economy index, allowing them to be compared with the cost on the same dimensional basis. The gain coefficient plays a crucial role in this transformation process, as it determines the rationality and accuracy of the evaluation. Specifically, the gain coefficient represents the economic impact associated with the reduction of per mass CO_2 emissions (CNY/Kg- CO_2). The calculation formula of the gain coefficient is as the follows:

$$G_{ain} = \frac{C_{ele}}{\beta} \tag{18}$$

$$C = LCCP \times G_{ain} + C_{total} \tag{19}$$

where:
G_{ain}: The economic impact associated with the reduction of per mass CO_2 emissions, CNY·kg^{-1};
C: Compare index, CNY.

4 Results and discussion
Based on the calculations and summarizations presented in the above section, this paper discusses the following four results: the heating/cooling performance of the HPAC system at different temperatures, the annual power consumption of each HPAC system in each objective city, the life carbon emission and life total cost.

And the recommended maps for HPAC system based four angles: annual power consumption, life carbon
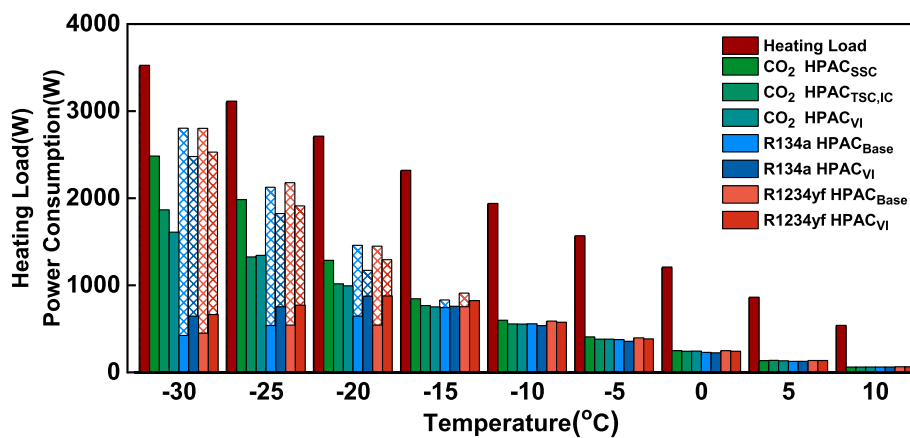

Fig. 7 The heating load and power consumption of each system at heating temperatures

Li *et al. Carbon Neutrality*   (2024) 3:16

Page 14 of 25

emissions, life total cost and comprehensive are showed in the section.

4.1 Heating/cooling performance of HPAC in each temperature

4.1.1 Heating performance

According to the above operating strategy, the heating load and power consumption of each system at each heating temperature are shown as Fig. 7.

During winter, the HVAC system is operated to deliver heat to the cabin maintaining the thermal comfort, resulting in the consumption of battery power. Figure 7 illustrates the power consumption and heating load of the HVAC systems under different heating temperatures and the dashed line indicates PTC heater heating energy consumption. Both the heating load and power consumption exhibit a gradient with respect to ambient temperature, indicating an increasing trend with decreasing temperature. Specifically, the highest heating load reaches 3550W at -30 ℃.

When the ambient temperature ranges from -15 to 10℃, the heating power consumption of the R134a systems is the lowest. However, due to the low thermal load demand in the cabin, there is no significant difference in the heating energy consumption among all HVAC systems within this temperature range; the maximum difference is only 41W. However, the heating capacity of R134a/R1234yf systems is inadequate for maintaining cabin temperature within the temperature range of -15 ℃ to -30 ℃, necessitating the utilization of a PTC heater for additional heat. As the ambient temperature decreases, the reliance on the PTC heater increases, accounting for approximately 67.8% of the heating load at -30 ℃. In contrast, the CO_2 systems can independently provide sufficient heating to meet the cabin heating requirements at all heating temperatures. The CO_2 systems demonstrated superior heating performance at -30~-15℃, reducing

heating energy consumption by 100 to 1188 W compared to the R134a and R1234yf systems.

In addition, the use of vapor injection and two-stage compression technology can significantly enhance the heating performance compared to the base system at lower ambient temperatures. The heating performance of the CO_2 $HPAC_{TSC,IC}$ and CO_2 $HPAC_{VI}$ systems showed a remarkable improvement of 34% and 43% at a temperature of -30 ℃. However, the benefit of these enhanced systems diminishes as the ambient temperature increases, with the improvement becoming less significant.

The COP serves as a performance index that incorporates both power consumption and heating load. A higher numerical value indicates superior performance. According to the results presented in Fig. 8, the COP of each HPAC system exhibited a decline as the ambient temperature decreased. This observation is consistent with the trend observed in Fig. 8. When the ambient temperature decreases, all systems experience a decline in performance due to the decreased evaporation pressure necessary for heat absorption from the surrounding environment and the Carnot cycle is less efficient.

Despite a decrease in COP across all systems, the extent of the decline varies, leading to superior performance within certain temperature ranges. Specifically, at temperatures ranging from -15 ℃ to -30 ℃, the COP of CO_2 $HPAC_{VI}$ is approximately 0.5 to 0.9 higher than that of R134a $HPAC_{Base}$. The impact of ambient temperature on the performance of each HPAC system can vary, resulting in differences in the magnitude of the decline in COP. Figure 8 provides a comparison of the COP of each system relative to the R134a HPAC $_{Base}$ system. Within the temperature range of -10 ℃ to -15 ℃, the COP of CO_2 systems outperforms that of the R134a $HPAC_{Base}$ system by approximately 0 to 1, indicating the suitability of CO_2 refrigerant for cold regions. However, in other
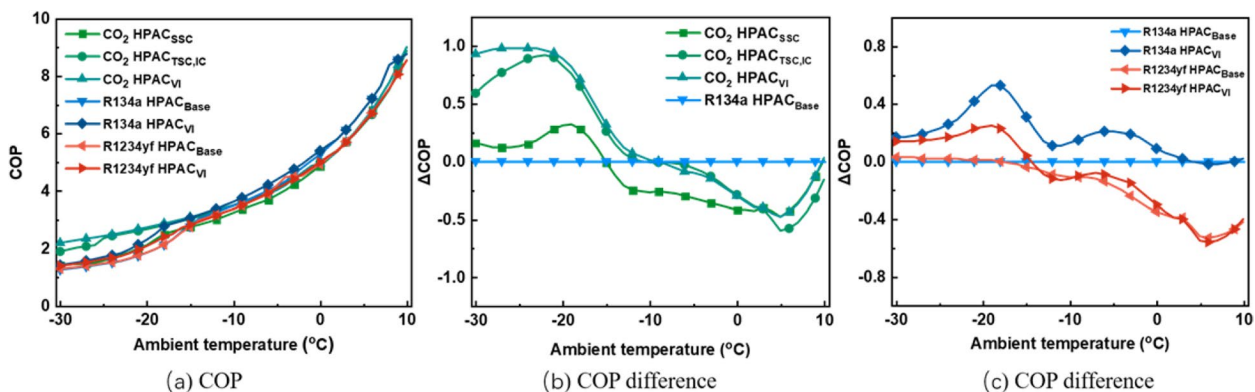

Fig. 8 The COP of each HPAC system at each heating temperature

Li *et al. Carbon Neutrality*   (2024) 3:16

Page 15 of 25
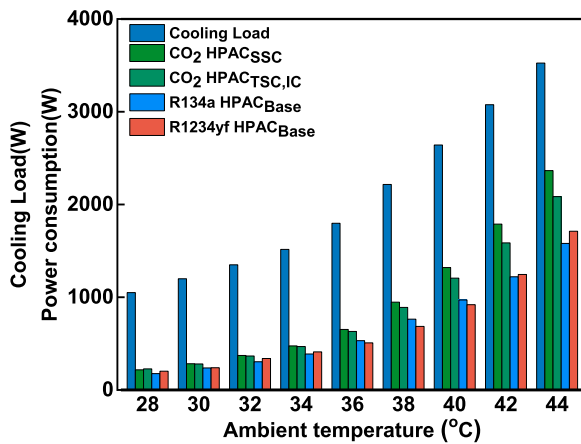
Fig. 9 The cooling load and energy consumption at each cooling temperature

heating temperature ranges, the R134a system exhibits superior performance. Additionally, the COP difference of the R1234yf refrigerant is minimal in the -30 ℃ to -5 ℃ temperature range, but it demonstrates lower performance at other temperatures.

In addition, the vapor injection and two-stage compression systems exhibit remarkable performance improvement and demonstrate a substantial boosting effect at low temperatures, resulting in an enhancement in COP of up to 0.2 ~ 0.6.

4.1.2 Cooling performance

Based on the above, the vapor injection branch was turned off in summer, resulting in a comparison of only four systems: namely CO_2 $HPAC_{SSC}$, CO_2 $HPAC_{TSC,\ IC}$,

R134a HPAC $_{Base}$, and R1234yf HPAC $_{Base}$. The cooling load and energy consumption of each system at different cooling temperatures are presented in Fig. 9. As shown in Fig. 9, as the ambient temperature increases, the cooling load and power consumption of each system also increase and the maximum cooling load reaches 3750W at 45 ℃. Additionally, at refrigeration temperatures, the power consumption of the CO_2 systems is approximately 5% to 40% higher than that of the R134a and R1234yf systems, suggesting that the cooling performance of CO_2 is inferior to that of the R134a and R1234yf systems. The two-stage compression technology demonstrates a power saving of approximately 4% to 13% compared to the base system.

In Fig. 10, the relationship between the ambient temperature and cooling COP variation of each HPAC system is presented. As the ambient temperature rises, the COP of each system decreases. Specifically, for R134a and R1234yf systems, an increase in ambient temperature leads to an increase in system condensing pressure and condensing temperature, resulting in a significant increase in pressure ratio, discharge temperature, and energy consumption, while the COP decreases. In contrast, for CO_2 systems, an rises in ambient temperature leads to an increase in the outlet temperature of the outdoor heat exchanger. This chain reaction triggers an increase in the optimal exhaust pressure, pressure ratio, discharge pressure, and energy consumption, while the COP similarly decreases.

Similar to heating, the rise in ambient temperature leads to a decline in the performance of the HPAC system, their decline trend is not the same. Figure 10 presents a comparison of the cooling performance of each system
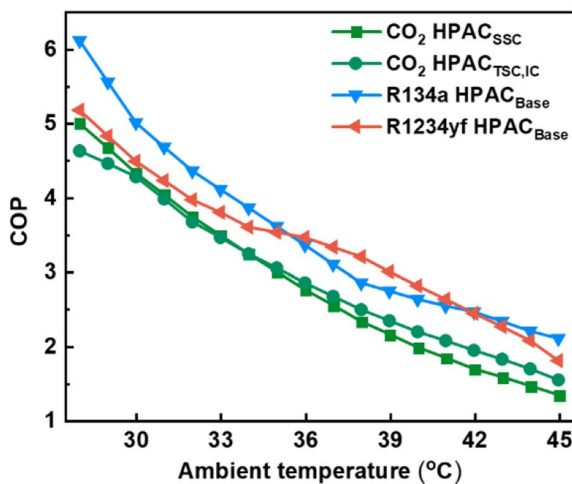
(a) COP
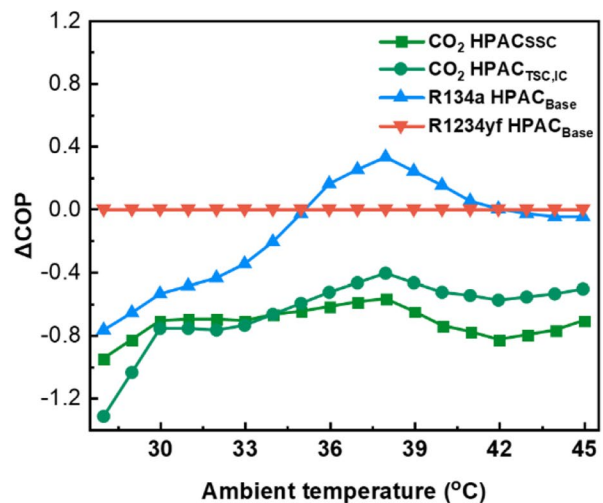
(b) COP difference

Fig. 10 Cooling COP difference of each HPAC systems at cooling temperatures

Li *et al. Carbon Neutrality*   (2024) 3:16

Page 16 of 25

based on the R134a HPAC $_{Base}$. The results indicate that the refrigeration performance of CO_2 systems is lower than that of R134a systems, which can be attributed to the inherent characteristics of CO_2. Furthermore, the COP of the CO_2 systems is approximately 0.5 to 1 lower than that of the R134a HPAC$_{Base}$ system. In contrast, for the R1234yf system, its cooling performance is better than that of the R134a system in the temperature range of 35 °C to 42 °C, while its cooling performance is lower than that of R134a at other temperatures.

4.2 The annual energy consumption in objective cities
4.2.1 The annual energy consumption in sample cities
As mentioned above, each HPAC system has its own advantage over different temperature intervals, and the climatic conditions of different cities vary due on their geographic dimensions. This variation leads to differing annual heating and cooling timeframes across cities. Therefore, identifying the most suitable system for each city requires a quantitative analysis of power consumption, environmental protection, and economic considerations.

The annual energy consumption of the HPAC systems serves as the comparative measure, and the findings are illustrated in Fig. 11 this study found that heat pump technology can significantly save energy, up to 1500 ~ 2000 kWh/year, in cold cities, such as Beijing, Moscow, and Washington. Conversely, the heat pump technology shows no significant impact in warm cities, such as Brasilia and Cairo. Although the differences in annual energy consumption among each heat pump system are relatively small, typically within a range of 10%.

And this study has identified the presence of an optimal system for each city. For example, while the R134a HPAC$_{VI}$ system exhibits the lowest annual power consumption among the systems, determining the most suitable system for each city and region based solely on annual energy consumption. Other factors such as annual carbon emissions and life cycle energy costs must also be considered.

4.2.2 The annual energy consumption in some objective cities
In order to further evaluate the annual energy consumption pattern of each HPAC system, this paper calculated the annual energy consumptions of each HPAC system across objective cities worldwide using the same method. Due to space limitations in this paper, the results of this analysis for elected cities are presented in Table 8.

Table 8 presents three typical scenarios, namely hot, warm and cold region, each with its own distinct characteristic. In hot regions like Port Moresby and Abuja, the difference in annual power consumption between the systems utilizing heat pump technology and those relying on PTC heaters during winter is negligible, typically around 50 kWh/year, rendering the heat pump technology ineffective in such regions.

In warm regions such as Washington and London, both heating and cooling demands need to be considered. Heat pump technology offers notable energy savings of up to 80% compared to PTC heaters. It is observed that the annual power consumption of CO_2 systems is higher compared to R134a and R1234yf systems. This disparity can be attributed to the fact that
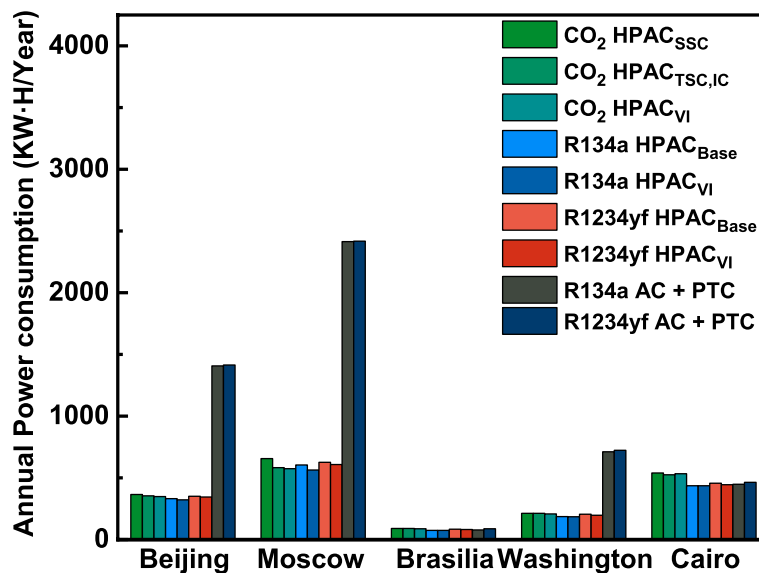
Fig. 11 Annual energy consumption of each system in sample cities

Table 8 The annual energy consumption of each system in some objective cities. (kWh/year)

		CO$_2$ HPAC$_{ssc}$	CO$_2$ HPAC$_{TSC,IC}$	CO$_2$ HPAC$_{VI}$	R134a HPAC$_{Base}$	R134a HPAC$_{VI}$	R1234yf HPAC$_{Base}$	R1234yf HPAC$_{VI}$	R134a AC+PTC	R1234yf AC+PTC
Hot region	Addis Ababa	0	0	0	0	0	0	0	1	1
	Bogotá	7	7	7	7	6	7	7	61	61
	Lubbock	100	102	100	84	84	95	90	91	101
	Hanoi	447	448	447	375	371	401	389	379	404
	Abuja	542	541	542	454	450	479	464	450	474
	Port Moresby	602	616	602	511	509	573	545	509	571
Warm region	Los Angeles	24	23	23	22	21	23	22	186	186
	Tokyo	155	155	150	136	133	148	142	522	531
	Washington	214	212	207	187	184	204	196	710	722
	London	132	127	123	120	116	127	122	834	835
	Stanley	186	179	174	170	163	179	172	1269	1269
	Hohhot	624	577	567	596	558	615	601	2320	2387
	Anchorage	731	647	639	662	621	681	670	2754	2754
Cold region	Amjertalik	2036	1557	1467	2028	1795	2025	1898	4947	4947
	Ekibastuz	3192	2288	2092	3247	2838	3209	2968	6015	6015
	Tura-Khansk	3767	2613	2326	3745	3325	3696	3430	6238	6239
	Hatanga	3862	2676	2394	3877	3422	3823	3539	6387	6388
	Sjansk	4083	2855	2556	4064	3606	4014	3728	6997	6998
	Yaroslavl	5781	3942	3481	5766	5112	5678	5258	8846	8847

Li *et al. Carbon Neutrality*   (2024) 3:16

Page 18 of 25

heating temperature in these regions does not reach extremely cold levels, thereby limiting the efficiency of CO_2 systems.

In cold regions like Tura-Khansk and Yaroslavl, the annual power consumption of those systems is significantly higher compared to the previous two regions. The CO_2 $HPAV_{VI}$ system exhibits significant potential for energy savings, ranging from 500 to 2000 kWh/year. This is attributed to its superior heating capabilities, particularly in extreme cold temperatures. The potential application of R1234yf $HPAC_{VI}$ systems appears unpromising for two reasons. First, in warm regions, it provides limited energy savings compared to the base system, as the heating temperature does not reach extreme cold levels. Second, in cold regions, the heating performance of the R1234yf $HPAC_{VI}$ system is significantly inferior to the CO_2 $HPAC_{VI}$ system.

A visualization map for the recommended system based on the annual power consumption is showed in the Fig. 12(a).

Each system exhibits distinct annual power consumption, and there exists a system with the minimum annual power consumption among them. After rigorous calculations and statistical analysis, the system demonstrating the lowest annual power consumption for each region is illustrated in Fig. 12(a). It is important to emphasize that the findings presented in Fig. 12(a) solely focus on the annual power consumption, and the advanced system consistently outperforms the base system, resulting in lower power consumption for the former. The CO_2 $HPAC_{VI}$ system, it is deemed more suitable for application in high latitude regions, as depicted by the green region in Fig. 12(a), for its superior heating performance. Conversely, the R134a $HPAC_{VI}$ system is found to be more suitable for the remaining regions, represented by the light grey region, given its performance characteristics. Therefore, it is not enough to consider the best suitable system only based on the annual power consumption.
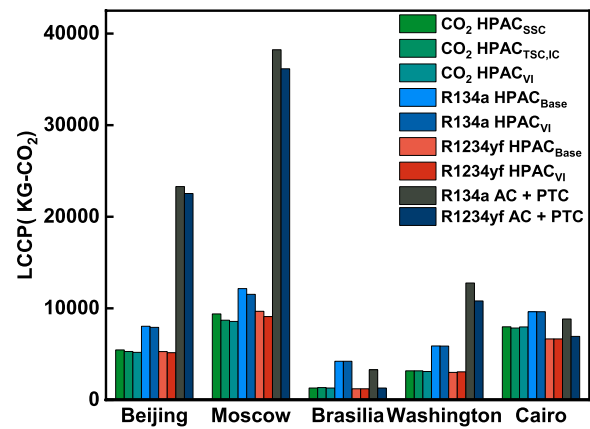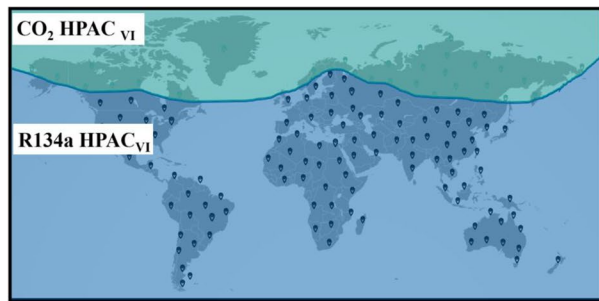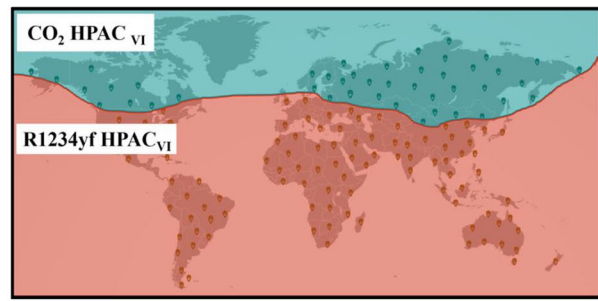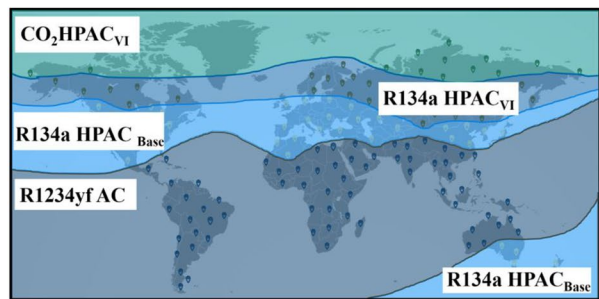

Fig. 13 The LCCP of each system in sample cities
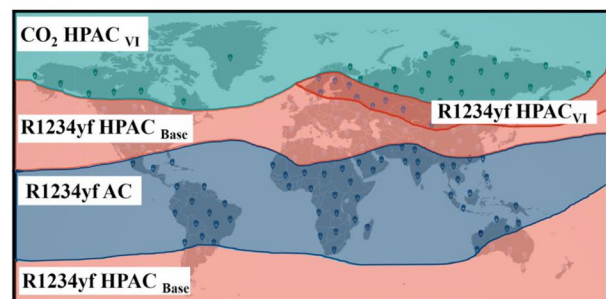

(a) the recommend system based on the power consumption

(b) the recommend system based on the LCCP

(c) the recommend system based on life total cost

(d) the recommend system based on the comprehensive analysis

Fig. 12 The recommend system map

4.3 The life carbon emission of each system in objective cities

4.3.1 The life carbon emission in sample cities
The source of LCCP associated with electric vehicle HPAC system can be divided into two categories: (1) LCCP caused by the refrigerant's own GWP and (2) LCCP caused by power consumption during operation. To assess the LCCP of HPAC system in the sample cities, This paper quantified the LCCP of both categories using established methods. Figure 13 shows the results of our analysis in sample, and it should be noted that the total amount of LCCP reported here represents the carbon emissions over the life cycle.

Figure 13 presents the LCCP of each system in sample cities. The results indicate that in regions such as Beijing, Moscow, and Washington, the R134a AC system generates significantly high carbon emissions about 23,174, 38,238 and 12,767 kg-CO_2, approximately 2 to 3 times higher than that of other systems, due to the large energy consumption required for PTC heating and the high GWP of R134a. Therefore, to reduce carbon emissions in such regions, adopting heat pump technology represents a highly promising approach. In warm regions, such as Brasilia and Cairo, the R134a systems are characterized by poor environmental performance due to GWP associated with R134a. Conversely, the R1234yf systems exhibit the best environmental performance in such regions.

4.3.2 The carbon emission in some objective cities
In order to further evaluate the LCCP of each system this study calculated these values for all targeted cities worldwide using the same method. Due to space limitations in the paper, the results for select cities are presented in Table 9.

The results presented in Table 9 indicate that R134a systems exhibit poor environmental performance in all regions due to its high GWP, which is a primary factor driving their eventual elimination. Specifically, in hot regions, the use of heat pump technology did not lead to a significant reduction in carbon emissions over traditional air-conditioning systems. However, in warm regions, heat pump technology demonstrated its advantage in reducing life cycle carbon emissions through decreased energy consumption and the HPAC system would releases more carbon emissions for the leakage of refrigerant. Finally, in cold regions, the CO_2 HPAC$_{VI}$ system exhibited the highest potential for promoting environmentally friendly performance, leading to carbon emission savings ranging from 20 to 60%. A visualization map for the recommended system based on the LCCP is showed in the Fig. 12(b).

From an environmental standpoint, Fig. 12(b) illustrates the system with the lowest LCCP. Despite not exhibiting superior performance, the R1234yf HPAC$_{VI}$ system is deemed more suitable for the low-middle latitude region, as indicated by the blue region in Fig. 12(b), owing to its low GWP. Conversely, the CO_2 HPAC$_{VI}$ system is found to be more suitable for high latitude regions.

4.4 The economic analysis of each system in objective cities

4.4.1 The initial investment cost of each system
The initial investment cost encompasses the expenses associated with all system components, and it should be noted that the component costs may vary for different refrigerants based on their operating parameters. Figure 14 illustrates the initial investment costs of each system. It is evident that the IIC of all CO_2 HPAC systems surpasses that of R134a systems by approximately 4000–10000 CNY, primarily due to the elevated cost of CO_2 compressors. At present, the CO_2 heat pump industry is still in its nascent stage of development, characterized by a lack of large-scale production of CO_2 compressors. Consequently, the current high prices of CO_2 compressors persist.

4.4.2 The life energy cost of each system in sample cities
As stated previously, the present study exclusively focuses on the analysis of life energy costs. The results obtained from the sample cities are presented in Fig. 15.

The life energy cost represents the cumulative electrical energy consumption over the service life of the system, which corresponds to the annual power consumption as depicted in Fig. 11. Figure 15 shows the life energy cost of each system in sample cities. It can be seen that the LEC of R134a and R1234yf AC systems is much larger—about 5 times greater—than that of other systems due to the inefficient PTC heater causing large energy consumption in Beijing, Moscow and Washington. The LEC of the HPAC systems demonstrates a saving effect.

4.4.3 The life total cost of each system in objective cities
The life total cost of each system in objective cities, including the IIC and the LEC, is expressed in the Table 10. Due to space limitations in the paper, the analysis results are presented.

In hot and warm regions, the life total cost of CO_2 systems is comparatively higher, ranging from 11,000 to 30,000 CNY, compared to other systems, this can be attributed to the expensive compressor used in CO_2 systems. However, in cold regions like Hatanga, CO_2 systems exhibit superior economic performance. In hot regions, systems without heat pump technology demonstrate the best economy performance, while in warm

Table 9 The life carbon emission of each system in some objective cities. (kg-CO_2)

	City	CO_2 HPAC$_{ssc}$	CO_2 HPAC$_{TSC,IC}$	CO_2 HPAC$_{VI}$	R134a HPAC$_{Base}$	R134a HPAC$_{VI}$	R1234yf HPAC$_{Base}$	R1234yf HPAC$_{VI}$	R134a AC+PTC	R1234yf AC+PTC
Hot region	Addis Ababa	6	7	6	3127	3127	21	21	2159	24
	Bogotá	113	109	107	3227	3220	126	118	3057	921
	Lubbock	1495	1532	1494	4385	4382	1432	1367	3504	1518
	Hanoi	6684	6704	6684	8730	8678	6019	5836	7812	6058
	Abuja	8107	8089	8107	9908	9849	7183	6956	8872	7096
	Port Moresby	9009	9211	9009	10,770	10,736	8581	8169	9760	8548
Warm region	Los Angeles	359	350	341	3455	3433	368	342	4927	2794
	Tokyo	2315	2313	2252	5150	5109	2226	2135	9956	7958
	Washington	3207	3179	3097	5926	5872	3062	2955	12,767	10,809
	London	1976	1903	1847	4921	4852	1912	1845	14,621	12,499
	Stanley	2783	2672	2598	5673	5564	2690	2589	21,128	18,992
	Hohhot	9341	8634	8489	12,042	11,468	9211	9008	36,843	35,704
	Anchorage	10,930	9676	9566	13,031	12,404	10,202	10,043	43,335	41,199
Cold region	Amjertalik	30,447	23,282	21,946	33,456	29,972	30,294	28,406	76,132	73,997
	Ekibastuz	47,743	34,216	31,286	51,689	45,569	48,011	44,402	92,108	89,974
	Tura-Khansk	56,339	39,080	34,788	59,136	52,846	55,290	51,318	95,430	93,313
	Hatanga	57,761	40,023	35,802	61,101	54,303	57,184	52,937	97,671	95,541
	Sjansk	61,061	42,700	38,233	63,895	57,047	60,048	55,772	106,791	104,669
	Yaroslavl	86,463	58,958	52,068	89,354	79,569	84,933	78,648	134,438	132,315

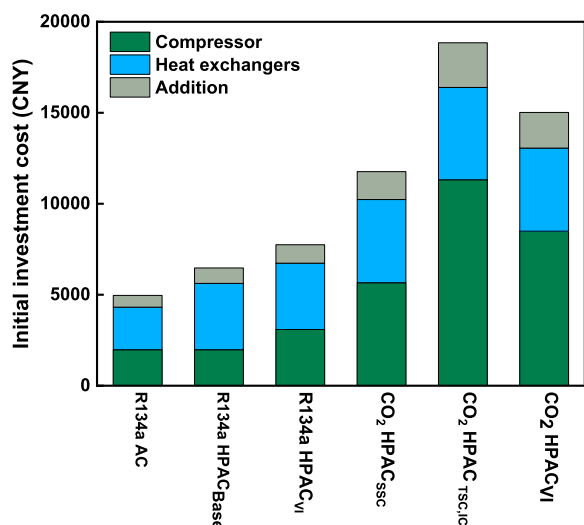Li *et al. Carbon Neutrality*   (2024) 3:16

Page 21 of 25

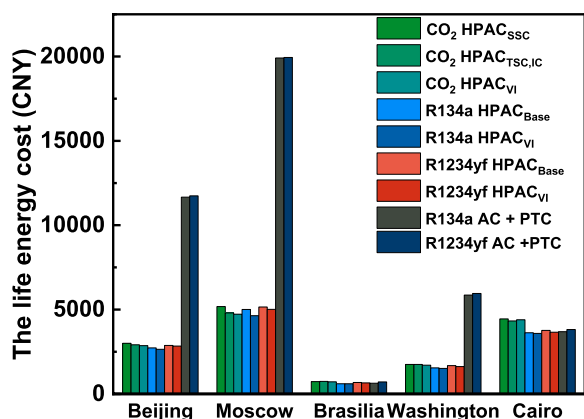**Fig. 14** The initial investment cost of each system

Fig. 15 The life energy cost of each system in sample cities

regions, the base heat pump systems exhibit the best economic performance.

From an economic perspective, Fig. 12 (c) shows the most cost-effective system across various regions worldwide. The results display a gradual change in gradients, recommending the R1234yf AC system for hot regions (indicated by the blue region), the R134a HPAC$_{Base}$ system for warm regions (represented by the pale yellow region), and the CO_2 HPACVI system for cold regions. For the transition region between warm and cold, the R134a HPACVI system is recommended.

4.5 The map of recommended HPAC system in objective cities

In order to determine the best-fit HPAC system for each region, a selection criterion based on the analysis results of annual energy consumption, life carbon emissions, and life energy cost should be applied. A comprehensive comparative index has been introduced as an evaluation criterion to evaluate systems, enabling the comparison of life carbon emissions and life energy costs on the unified dimensional scale by incorporating the concept of transforming carbon emissions into an economic index. The statistical result of the compare index of certain objective cities is shows in the Table 11. The suitability of the system inversely correlates with the comparative index value, meaning that a smaller comparative index indicates a more suitable system. The visualization result all around the world is showed in the Fig. 12(d).

According to the results presented in Fig. 12(d), the CO_2 HPAC$_{VI}$ system is recommended for cold regions to meet both environmental and economic criteria, as the green part showed. In this region, annual energy consumption is the primary consideration. The R1234yf HPAC$_{Base}$ system is recommended for warm regions where extreme weather conditions are not prevalent, as the baby blue part showed. For regions transitioning from cold to warm climates, the R1234yf HPAC$_{VI}$ system is suggested, as the deep blue part showed. And Both environmental performance and annual energy consumption of the refrigerant are considered. In hot regions, the R1234yf AC system is recommended. The environmental protection of the refrigerant can be a major consideration. These recommendations are based on quantification of annual power consumption, life cycle climate performance, andeconomic analysis ensuring a suitable system choice for each region worldwide.

5 Conclusion

This study aimed to determine the optimal HVAC systems for PBEVs by conducting quantitative assessments on three key factors: annual energy consumption, life cycle carbon emissions, and life total costs. The analysis was carried out across multiple regions worldwide. By considering the combined influence of these three factors, the most suitable and efficient HVAC system was identified for PBEVs in each specific region. These findings provide valuable insights for the development and implementation of sustainable heat pump technologies in the automotive industry, promoting the advancement of environmentally friendly PBEVs.

The main conclusions of this paper are as follows:

When the ambient temperature ranges from -15 to 10℃, the R134a system exhibits the lowest heating energy consumption. However, across the various HVAC systems, there's no significant difference in heating energy consumption within this temperature range, with the maximum difference being only 41W. In the colder temperature range of -30 to -15℃, the CO_2 system outperforms the R134a and R1234yf systems, showing an improvement of up to 0.9 in its COP compared to the

Li *et al. Carbon Neutrality* (2024) 3:16

Page 22 of 25

Table 10 The total cost of each system in some objective cities. (CNY)

		CO_2 HPAC$_{ssc}$	CO_2 HPAC$_{TSC,IC}$	CO_2 HPAC$_{VI}$	R134a HPAC$_{Base}$	R134a HPAC$_{VI}$	R1234yf HPAC$_{Base}$	R1234yf HPAC$_{VI}$	R134a AC+PTC	R1234yf AC+PTC
Hot region	Addis Ababa	11,769	18,853	15,024	6473	7751	6474	7751	4980	4978
	Bogotá	11,897	18,977	15,145	6593	7862	6600	7867	6060	6059
	Lubbock	13,560	20,689	16,815	7987	9261	8171	9371	6779	6598
	Hanoi	19,807	26,914	23,061	13,216	14,432	13,692	14,749	12,243	11,783
	Abuja	23,977	28,581	24,774	14,635	15,841	15,094	16,097	13,493	13,059
	Port Moresby	22,604	29,932	25,859	15,672	16,909	16,777	17,558	15,240	14,127
Warm region	Los Angeles	12,193	19,266	15,427	6868	8119	6891	8136	8315	8311
	Tokyo	14,548	21,630	17,727	8908	10,137	9127	10,295	14,530	14,363
	Washington	15,621	22,672	18,744	9842	11,054	10,133	11,282	17,962	17,747
	London	14,140	21,135	17,239	8633	9828	8749	9946	19,995	19,979
	Stanley	15,111	22,061	18,143	9538	10,684	9686	10,841	27,811	27,810
	Hohhot	23,004	29,237	25,234	17,202	17,790	17,534	18,567	47,925	46,725
	Anchorage	24,916	30,491	26,530	18,394	18,917	18,727	19,813	54,539	54,538
Cold region	Amjertalik	48,407	46,868	41,430	42,977	40,062	42,911	41,915	94,015	94,014
	Ekibastuz	69,225	60,028	52,673	64,922	58,835	64,235	61,168	113,245	113,243
	Tura-Khansk	79,572	65,882	56,888	73,886	67,593	72,995	69,492	117,264	117,241
	Hatanga	81,282	67,018	58,107	76,252	69,347	75,275	71,441	119,945	119,938
	Sjansk	85,254	70,239	61,033	79,613	72,649	78,722	74,853	130,932	130,915
	Yaroslavl	115,829	89,808	77,686	110,257	99,758	108,674	102,387	164,208	164,192

Table 11 The compara index of each system in some objective cities. (CNY)

		CO$_2$ HPAC	CO$_2$ HPAC$_{TSC,IC}$	CO$_2$ HPAC$_{VI}$	R134a HPAC$_{Base}$	R134a HPAC$_{VI}$	R1234yf HPAC$_{Base}$	R1234yf HPAC$_{VI}$	R134a AC+PTC	R1234yf AC+PTC
Hot region	Addis Ababa	11,779	18,864	15,034	11,333	12,611	6507	7784	8335	5015
	Bogotá	12,072	19,146	15,310	11,608	12,865	6796	8050	10,811	7491
	Lubbock	15,883	23,069	19,136	14,802	16,071	10,396	11,496	12,225	8957
	Hanoi	30,194	37,332	33,447	26,783	27,916	23,046	23,818	24,383	21,197
	Abuja	34,118	41,152	37,373	30,032	31,146	26,257	26,907	27,280	24,087
	Port Moresby	36,604	44,246	39,859	32,409	33,593	30,112	30,253	30,407	27,411
Warm region	Los Angeles	12,750	19,809	15,957	12,236	13,453	7463	8668	15,972	12,653
	Tokyo	18,146	25,225	21,228	16,912	18,077	12,586	13,613	30,001	26,730
	Washington	20,605	27,612	23,558	19,050	20,179	14,891	15,874	37,802	34,545
	London	17,211	24,092	20,109	16,280	17,368	11,720	12,813	42,717	39,401
	Stanley	19,436	26,213	22,181	18,354	19,330	13,866	14,864	60,644	57,324
	Hohhot	37,519	42,654	38,426	35,915	35,611	31,847	32,566	105,180	102,209
	Anchorage	41,901	45,527	41,395	38,644	38,194	34,580	35,420	121,881	118,561
Cold region	Amjertalik	95,721	83,048	75,534	94,967	86,640	89,988	86,058	212,325	209,005
	Ekibastuz	143,416	113,199	101,291	145,246	129,649	138,844	130,169	256,381	253,062
	Tura-Khansk	167,123	126,612	110,948	165,784	149,716	158,915	149,241	265,563	262,249
	Hatanga	171,043	129,214	113,743	171,203	153,733	164,140	153,706	271,726	268,408
	Sjansk	180,143	136,594	120,447	178,905	161,300	172,037	161,523	296,885	293,570
	Yaroslavl	250,193	181,430	158,600	249,113	223,409	240,661	224,606	373,125	369,810

Li *et al. Carbon Neutrality*   (2024) 3:16

Page 24 of 25

R134a HPAC$_{Base}$. At cooling temperatures, however, the power consumption of the CO_2 systems is approximately 5% to 40% higher than that of the R134a and R1234yf systems.

From an annual energy consumption perspective, heat pump technology demonstrates significant potential for energy savings in both warm and cold regions. Comparatively, heat pump technology offers remarkable energy savings of up to 80% compared to PTC heaters in Washington and London. In addition, the energy consumption of each heat pump system is comparable in warm regions, whereas there is a significant disparity in energy consumption in cold regions.

Considering the life cycle climate performance, the R134a systems demonstrate the lowest environmental performance across all regions due to their high GWP. On the other hand, the CO_2 HPAC$_{VI}$ system displays exceptional environmental friendliness, especially in cold regions, leading to carbon emission savings ranging from 20 to 60%.

From the life cycle economic perspective, the cost of compressors in CO_2 systems represents a significant portion of the initial investment cost, surpassing that of R134a and R1234yf systems. This cost differential acts as a primary hindrance to expanding the application potential of CO_2 systems in warm region.

Based on the quantitative computation evaluation of annual energy consumption, life cycle climate performance and life total cost, this study proposes a comprehensive selection map for air conditioning systems in electric vehicles. In the hot region, the R1234yf AC system is recommended to be used for better environmental performance. In the warm region, the R1234yf HPAC $_{Base}$ system is recommended to be used. In the cold region, the CO_2 HPAC$_{VI}$ is recommended. For regions transitioning from cold to warm climates, the R1234yf HPAC$_{VI}$ system is suggested. The map can be as a selection reference and decision-making for the air-condition system of electric vehicles.

Abbreviations

AC	Air-Conditioning
ACCU	Accumulator
COM	Compressor
COP	Coefficient Of Performance
UTC	Coordinated Universal Time
EVA	Evaporator
EEV	Electronic Expansion Valve
GHG	Greenhouse gas
GWP	Global Warming Potential
HPAC	Heat Pump Air Conditioning
LCCP	Life Cycle Climate Performance
ICEV	Internal Combustion Engine Vehicle
IIC	Initial Investment Cost
IEC	Life Energy Cost
OHX	Outdoor Heat Exchanger
PTC	Positive Temperature Coefficient
PBEV	Pure Battery Electric Vehicle
PID	Proportional-Integral-Derivative

Availability of data and materials
The original data are available form corresponding authors upon reasonable request.

Declarations

Ethics approval and consent to participate
The manuscript is original and not submitted to other journal, all the results are without fabrication. The authors consent to participate in the manuscript.

Consent for publication
Not applicable.

Competing interests
The authors declare that they have no known competing financial interests or personal relationships that could have appeared to influence the work reported in this paper.

References
1. Kamandika FA, Dhakal S (2023) Impact of carbon price on Indonesia's power sector up to 2050. Carbon Neutrality 2:27
2. Zhou Y, Li J, Cui J, Wang H, Wang C, Zhang R et al (2023) Personal GHG emissions accounting and the driving forces decomposition in the past 10 years. Carbon Neutrality 2:3
3. Zhuang W, Li S, Zhang X, Kum D, Song Z, Yin G et al (2020) A survey of powertrain configuration studies on hybrid electric vehicles. Applied Energy 262:114553
4. Park MH, Kim SC (2019) Heating Performance Enhancement of High Capacity PTC Heater with Modified Louver Fin for Electric Vehicles. Energies 12:2900
5. Zhang Z, Li W, Zhang C, Chen J (2017) Climate control loads prediction of electric vehicles. Appl Therm Eng 110:1183–1188
6. Qi Z (2014) Advances on air conditioning and heat pump system in electric vehicles - A review. Renew Sustain Energy Rev 38:754–764
7. Illán-Gómez F, López-Belchí A, García-Cascales JR, Vera-García F (2015) Experimental two-phase heat transfer coefficient and frictional pressure drop inside mini-channels during condensation with R1234yf and R134a. Int J Refrig 51:12–23

Li *et al. Carbon Neutrality*   (2024) 3:16

Page 25 of 25

8. Sarkar J (2013) Transcritical CO_2 Refrigeration Systems: Comparison with Conventional Solutions and Applications. International Journal of Air-Conditioning and Refrigeration 20:1250017

9. Wang H, Bi H, Zhou Y, Li C (2020) Field measurements and numerical analysis of the energy consumption of urban rail vehicle air-conditioning systems. Appl Therm Eng 177:115497

10. Yang T, Zou H, Tang M, Tian C, Yan Y (2022) Experimental performance of a vapor-injection CO_2 heat pump system for electric vehicles in −30 °C to 50 °C range. Appl Therm Eng 217:119149

11. Peng F, Wei M, Huang H (2014) Effects of different ambient temperatures on performance of electric vehicles' heat pump air conditioning. Journal of Beijing University of Aeronautics and Astronautics 12:1741–1746

12. Lee H-S, Lee M-Y (2016) Steady state and start-up performance characteristics of air source heat pump for cabin heating in an electric passenger vehicle. Int J Refrig 69:232–242

13. Ciconkov R (2018) Refrigerants: There is still no vision for sustainable solutions. Int J Refrig 86:441–448

14. Li W, Liu R, Liu Y, Wang D, Shi J, Chen J (2020) Performance evaluation of R1234yf heat pump system for an electric vehicle in cold climate. Int J Refrig 115:117–125

15. Li Z, Khajepour A, Song J (2019) A comprehensive review of the key technologies for pure electric vehicles. Energy 182:824–839

16. Zou HM, Huang GY, Shao SQ, Zhang XQ, Tian CQ, Zhang XL (2017) Experimental Study on Heating Performance of an R1234yf Heat Pump System for Electric Cars. Enrgy Proced 142:1015–1021

17. Lee Y, Jung D (2012) A brief performance comparison of R1234yf and R134a in a bench tester for automobile applications. Appl Therm Eng 35:240–242

18. Bansal P (2012) A review – Status of CO_2 as a low temperature refrigerant: Fundamentals and R&D opportunities. Appl Therm Eng 41:18–29

19. Dai B, Li M, Ma Y (2014) Thermodynamic analysis of carbon dioxide blends with low GWP (global warming potential) working fluids-based transcritical Rankine cycles for low-grade heat energy recovery. Energy 64:942–952

20. Junqi D, Yibiao W, Shiwei J, Xianhui Z, Linjie H (2021) Experimental study of R744 heat pump system for electric vehicle application. Appl Therm Eng 183:116191

21. Wang D, Yu B, Hu J, Chen L, Shi J, Chen J (2018) Heating performance characteristics of CO_2 heat pump system for electrical vehicle in a cold climate. Int J Refrig 85:27–41

22. Brown JS (2001) Comparitive analysis of an automotive air conditioning systems operating with CO_2 and R134a. International Journal of Refrigeration. 25:19–32

23. Aprea C, Greco A, Maiorino A (2013) The substitution of R134a with R744: An exergetic analysis based on experimental data. Int J Refrig 36:2148–2159

24. Li Z, Liang K, Jiang H (2019) Experimental study of R1234yf as a drop-in replacement for R134a in an oil-free refrigeration system. Appl Therm Eng 153:646–654

25. Wang C, Cao F, Li M, Yin X, Song Y, He Y (2021) Research status and future development of thermalmanagement system for new energy vehicles underthe background of carbon neutrality. Chin Sci Bull 66:4112–4128

26. Prabakaran R, Lal DM, Kim SC (2022) A state of art review on future low global warming potential refrigerants and performance augmentation methods for vapour compression based mobile air conditioning system. J Therm Anal Calorim 148:417–449

27. Wu J, Zhou G, Wang M (2020) A comprehensive assessment of refrigerants for cabin heating and cooling on electric vehicles. Applied Thermal Engineering. 174:115258

28. Direk M, Yüksel F (2019) Experimental Evaluation of an Automotive Heat Pump System with R1234yf as an Alternative to R134a. Arab J Sci Eng 45:719–728

29. Wang Y, Dong J, Jia S, Huang L (2021) Experimental comparison of R744 and R134a heat pump systems for electric vehicle application. Int J Refrig 121:10–22

30. Song Y, Wang H, Ma Y, Yin X, Cao F (2022) Energetic, economic, environmental investigation of carbon dioxide as the refrigeration alternative in new energy bus/railway vehicles' air conditioning systems. Applied Energy. 305:117830

31. Liu S, Li Z, Dai B, Zhong Z, Li H, Song M et al (2019) Energetic, economic and environmental analysis of air source transcritical CO_2 heat pump system for residential heating in China. Appl Therm Eng 148:1425–1439

32. Cho H, Baek C, Park C, Kim Y (2009) Performance evaluation of a two-stage CO_2 cycle with gas injection in the cooling mode operation. Int J Refrig 32:40–46

33. Peng X, Wang D, Wang G, Yang Y, Xiang S (2020) Numerical investigation on the heating performance of a transcritical CO_2 vapor-injection heat pump system. Applied Thermal Engineering. 166:114656

34. Wang H, Ji Z, Wang C, Zhu Z, Wang Y, Lin H (2022) Experimental study of propane heat pump system with secondary loop and vapor injection for electric vehicle application in cold climate. Applied Thermal Engineering. 217:119196

35. Chen Y, Zou H, Dong J, Wu J, Xu H, Tian C (2021) Experimental investigation on the heating performance of a CO_2 heat pump system with intermediate cooling for electric vehicles. Applied Thermal Engineering. 182:116039

36. Jung U, Jeon Y, Lee H, Kim Y (2017) Numerical study of the effects of injection-port design on the heating performance of an R134a heat pump with vapor injection used in electric vehicles. Appl Therm Eng 127:800–811

37. Liu X, Hu Y, Wang Q, Yao L, Li M (2021) Energetic, environmental and economic comparative analyses of modified transcritical CO_2 heat pump system to replace R134a system for home heating. Energy. 229:120544

38. Qureshi BA, Zubair SM (2011) Performance degradation of a vapor compression refrigeration system under fouled conditions. Int J Refrig 34:1016–1027

39. de Paula CH, Duarte WM, Rocha TTM, de Oliveira RN, Maia AAT (2020) Optimal design and environmental, energy and exergy analysis of a vapor compression refrigeration system using R290, R1234yf, and R744 as alternatives to replace R134a. Int J Refrig 113:10–20

40. Yang D, Song Y, Cao F, Jin L, Wang X (2016) Theoretical and experimental investigation of a combined R134a and transcritical CO_2 heat pump for space heating. Int J Refrig 72:156–170

41. Song Y, Cao F (2018) The evaluation of optimal discharge pressure in a water-precooler-based transcritical CO_2 heat pump system. Appl Therm Eng 131:8–18

42. Gnielinski V (1976) New equations for heat and mass-transfer in turbulent pipe and channel flow. Int Chem Eng 16:359–368

43. Shah MM (1979) General correlation for heat-transfer during film condensation inside pipes. Int J Heat Mass Transf 22:547–556

44. Wang D, Yu B, Li W, Shi J, Chen J (2018) Heating performance evaluation of a CO_2 heat pump system for an electrical vehicle at cold ambient temperatures. Appl Therm Eng 142:656–64

45. Wu X, Hu S, Mo S (2013) Carbon footprint model for evaluating the global warming impact of food transport refrigeration systems. J Clean Prod 54:115–124

46. Hafner A, Försterling S, Banasiak K (2014) Multi-ejector concept for R-744 supermarket refrigeration. Int J Refrig 43:1–13

47. Changru Yang SS (2021) Nobuo Takata, Kyaw Thu, Takahiko Miyazaki The life cycle climate performance evaluation of low-GWP refrigerantsfor domestic heat pumps. Int J Refrig 121:33–42

48. Fazelpour F, Morosuk T (2014) Exergoeconomic analysis of carbon dioxide transcritical refrigeration machines. Int J Refrig 38:128–139

Publisher's Note